

## Stability, electronic and magnetic properties, and reactivity of icosahedral $MCo_{12}$ clusters

Yang Jinlong

*Chinese Center of Advanced Science and Technology (World Laboratory), P.O. Box 8730, Beijing 100080, China  
and Center for Fundamental Physics, University of Science and Technology of China, Hefei, Anhui 230026, People's Republic of China\**

Xiao Chuanyun

*Department of Physics, Huazhong Normal University, Wuhan, Hubei 430070, People's Republic of China*

Xia Shangda

*Department of Physics, University of Science and Technology of China, Hefei, Anhui 230026, People's Republic of China*

Wang Kelin

*Center for Fundamental Physics, University of Science and Technology of China, Hefei, Anhui 230026, People's Republic of China*

(Received 25 January 1993; revised manuscript received 13 July 1993)

The stability, electronic and magnetic properties, and reactivity of icosahedral  $MCo_{12}$  clusters are studied using the discrete variational local-spin-density-functional method, where  $M = Ti, V, Cr, Mn, Fe, Co,$  and  $Ni$ . By means of the binding-energy calculation, we obtained the  $M$ -Co bond length of the clusters and compared their relative stability. We calculated the electronic structure of the clusters in their equilibrium configurations. The calculated results show that all the clusters have metallic character, and that the clusters with  $M$  being  $Ti, Mn,$  or  $Co$  have closed electronic shells while the others have open electronic shells and are expected to distort further. The results also indicate that the cluster moment is reduced by the substitution of the central  $Co$  atom with an  $M$  atom, and that the average moment per atom of all clusters is larger than that of the bulk  $Co$ . Based on the results of electronic structures, we further analyzed the reactivity of the clusters toward  $H_2, N_2,$  and  $CO$  molecules and found a strong dependence on the central  $M$  atom. Our results compare well with the available experimental results.

### I. INTRODUCTION

Recently, there has been extensive interest in metal clusters containing several to dozens of atoms.<sup>1</sup> This is not only because the intrinsic electronic, optical, magnetic, and structural properties of such clusters are of fundamental importance in exploring new cluster-based materials with uncommon properties, but also because such clusters may serve as models for understanding localized electronic phenomena in metals.

Early investigations on metal clusters are largely confined to genuine clusters composed of only one element.<sup>2,3</sup> To increase the number of variables for the purpose of material design and control, metal clusters composed of two or more elements have been attracting increasing attention. The properties of such clusters depend not only on the cluster size and geometry, as is the case for genuine clusters, but also on the cluster composition. Many bimetallic clusters have been generated by the crucible method or modified laser vaporization technique, and the mass distribution, reactivity, and stability of them have been measured.<sup>4,5</sup> Theoretically, Petterson and Bauschlicher<sup>6</sup> studied the effect of impurities on the binding energy and structure of small  $Al$  and  $Be$  clusters; Dunlap<sup>7</sup> studied the influence of symmetry on the magnetism of  $Fe_{12}X$ , while Khanna and Jena<sup>8</sup> studied the stability of  $Al_{12}X$  clusters and the interaction between two such clusters. All of these studies show that structures and properties of the clusters can be changed by means of

doping.

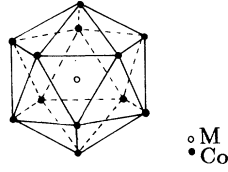
Binary transition-metal clusters are of significant interest, due to their promising practical applications in developing new magnetic materials with large moments and new catalysts with high reactivity.<sup>9-11</sup> For binary  $Co-M$  clusters, some experiments have been carried out on their ionization potentials<sup>12</sup> and reactivity.<sup>13-16</sup> However, there are few theoretical studies for them.

In this paper, we performed a comprehensive first-principles study on  $MCo_{12}$  clusters in the hope of examining the effect of the impurity  $M$  on the stability, electronic and magnetic properties, and reactivity of the clusters, where  $M = Ti, V, Cr, Mn, Fe, Co,$  and  $Ni$ . The paper is arranged as follows: the cluster models and computational parameters are described in Sec. II; our results and discussions are presented in Sec. III; finally, a summary is given in Sec. IV.

### II. CLUSTER MODELS AND COMPUTATIONAL PARAMETERS

Since previous studies<sup>17,18</sup> on metal clusters have shown that the icosahedral structure for a 13-atom metal cluster is the most energetically stable, we assume that all of our  $MCo_{12}$  clusters have an icosahedral point-group symmetry with  $M$  at the center of the icosahedron. The geometry of an icosahedral  $MCo_{12}$  cluster is shown in Fig. 1.

The discrete-variational local-spin-density-functional

FIG. 1. Geometry of an icosahedral  $M\text{Co}_{12}$  cluster.

(DV-LSD) method is used in our calculations. It is a kind of molecular-orbital calculation method and its theoretical foundation is the LSD theory. As it has been described in detail elsewhere,<sup>19–21</sup> we do not give a further description here. In our calculations, the exchange-correlation potential is taken to be of the von Barth–Hedin form,<sup>22</sup> in which the necessary parameters are chosen to agree with those of Moruzzi, Janak, and Williams;<sup>23</sup> the numerical atomic basis functions are chosen as the variational basis set, i.e., the  $1s-4p$  of a  $M$  atom within a spherical potential well of radius 6 a.u. and depth 2.0 a.u.; lower-energy orbitals ( $M 1s-3p$ ) are treated as frozen cores and the number of the Diophantus sample points is 3900; and the convergence accuracy of the self-consistent charge process is  $10^{-4}e$ .

### III. RESULTS AND DISCUSSIONS

#### A. Binding energy and stability of icosahedral $M\text{Co}_{12}$ clusters

To obtain the result of electronic structure calculations, one should first of all know the equilibrium geometrical parameters of a cluster. For icosahedral  $M\text{Co}_{12}$  clusters, the only geometrical parameter is the bond length between the central  $M$  and surface Co atoms. We calculate the total binding energy for each  $M\text{Co}_{12}$  cluster at several internuclear configurations and, by maximizing the total binding energy, determine the equilibrium bond length  $r_{M-\text{Co}}$  as presented in Table I. For comparison with the bulk counterpart, Table I lists the sum ( $r_M + r_{\text{Co}}$ ) of the radii for  $M$  and Co atoms. Obviously,  $r_{M-\text{Co}} < r_M + r_{\text{Co}}$  for all  $M$ 's. This means that there is a bond-length contraction effect in all clusters. We take  $\text{CoCo}_{12}$  as an example. The bond length between the cen-

TABLE I. The equilibrium bond lengths and binding energies for icosahedral  $M\text{Co}_{12}$  clusters.  $\Delta E_b = E_b(M\text{Co}_{12}) - E_b(\text{CoCo}_{12})$ .

Cluster	$r_{M-\text{Co}}$ (a.u.)	$r_M + r_{\text{Co}}$ (a.u.)	$E_b$ (eV)	$\Delta E_b$ (eV)
$\text{TiCo}_{12}$	4.5	5.1	90.91	1.53
$\text{VCo}_{12}$	4.4	4.8	92.31	2.93
$\text{CrCo}_{12}$	4.4	4.7	93.80	4.42
$\text{MnCo}_{12}$	4.5	4.9	92.10	2.72
$\text{FeCo}_{12}$	4.4	4.7	90.70	1.32
$\text{CoCo}_{12}$	4.4	4.7	89.38	0.00
$\text{NiCo}_{12}$	4.4	4.7	87.92	-1.46

tral and surface Co atoms is 4.4 a.u., which is 7% shorter than that of 4.7 a.u. in a fcc Co crystal.<sup>24</sup> Such a contraction effect was observed by extended x-ray-absorption fine structure<sup>25</sup> in Cu and Ni clusters and the contraction ratio was found to be proportional to the surface-to-volume ratio of the cluster, so this effect is believed to be a reflection of surface effects.

Table I also lists the binding energies of  $M\text{Co}_{12}$  clusters in their respective equilibrium configurations. Although the equilibrium bond lengths are almost the same for all clusters, their binding energies are appreciably distinct. By comparing the difference  $\Delta E_b$ , which is defined as the binding energy of  $M\text{Co}_{12}$  subtracted that of the  $\text{CoCo}_{12}$  cluster, we can examine the relative stability between the genuine  $\text{CoCo}_{12}$  and doped  $M\text{Co}_{12}$  clusters. From Table

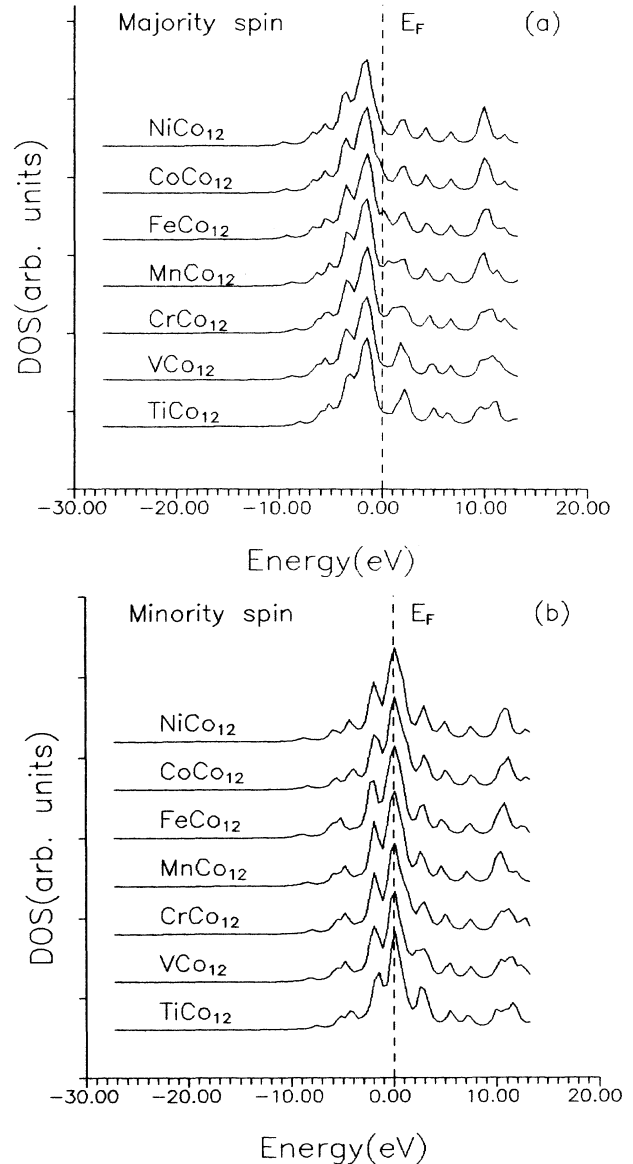


FIG. 2. DOS for icosahedral  $M\text{Co}_{12}$  clusters: (a) majority spin and (b) minority spin.

TABLE II. The data of electronic structure for icosahedral  $M\text{Co}_{12}$  clusters (eV).

Cluster	VBW	HOMO	LUMO	$E_F$
TiCo <sub>12</sub>	8.00	-3.78	-3.62	-3.70
VCo <sub>12</sub>	8.81	-3.82	-3.82	-3.82
CrCo <sub>12</sub>	8.54	-3.69	-3.69	-3.69
MnCo <sub>12</sub>	8.75	-3.74	-3.63	-3.69
FeCo <sub>12</sub>	9.32	-3.70	-3.70	-3.70
CoCo <sub>12</sub>	9.36	-3.94	-3.77	-3.85
NiCo <sub>12</sub>	9.63	-3.82	-3.82	-3.82

I, we see that CrCo<sub>12</sub> is the most energetically stable among all the  $M\text{Co}_{12}$  clusters, and doped  $M\text{Co}_{12}$  clusters, except for NiCo<sub>12</sub>, are more stable than the CoCo<sub>12</sub> cluster.

We obtain the binding energy to be 6.88 eV/atom for a CoCo<sub>12</sub> cluster, which is considerably greater than that of 4.4 eV/atom for a fcc Co crystal.<sup>22</sup> This indicates that interactions are strengthened among atoms in CoCo<sub>12</sub> cluster because of the bond-length contraction.

#### B. Electronic and magnetic properties of icosahedral $M\text{Co}_{12}$ clusters

With the equilibrium bond lengths obtained above, we further calculate the electronic and magnetic properties of icosahedral  $M\text{Co}_{12}$  clusters. The main results are presented in Figs. 2–4 and Tables II–V.

Figures 2(a) and 2(b) present the densities of states (DOS's) for the majority- and minority-spin electrons in  $M\text{Co}_{12}$  clusters, respectively, which are obtained<sup>26</sup> by a Lorentzian extension of the discrete energy levels and a summation over them. Since the DOS's for all  $M\text{Co}_{12}$  clusters look similar, we first analyze the DOS for the

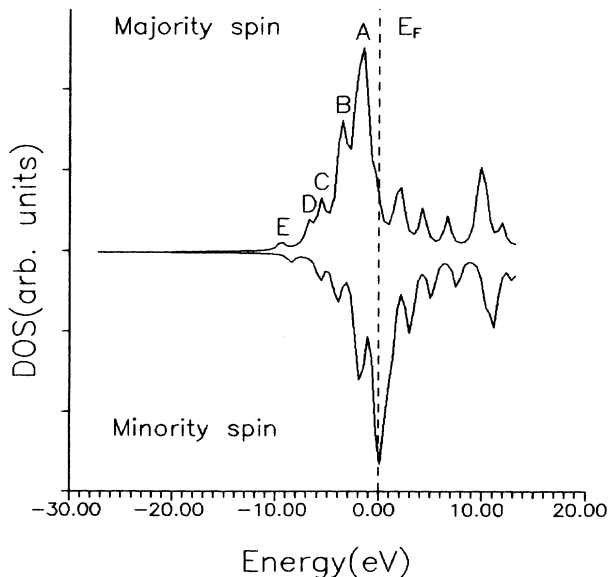


FIG. 3. DOS for an icosahedral CoCo<sub>12</sub> cluster.

TABLE III. The ground-state electronic configurations for icosahedral  $M\text{Co}_{12}$  clusters.

Cluster	HOMO		Electronic configuration
	Symbol	Electrons	
TiCo <sub>12</sub>	$2g_u \downarrow$	4	closed
VCo <sub>12</sub>	$3t_{1u} \downarrow$	1	open
CrCo <sub>12</sub>	$3t_{1u} \downarrow$	2	open
MnCo <sub>12</sub>	$3t_{1u} \downarrow$	3	closed
FeCo <sub>12</sub>	$2g_g \downarrow$	1	open
CoCo <sub>12</sub>	$2g_u \downarrow$	4	closed
NiCo <sub>12</sub>	$3t_{1u} \downarrow$	1	open

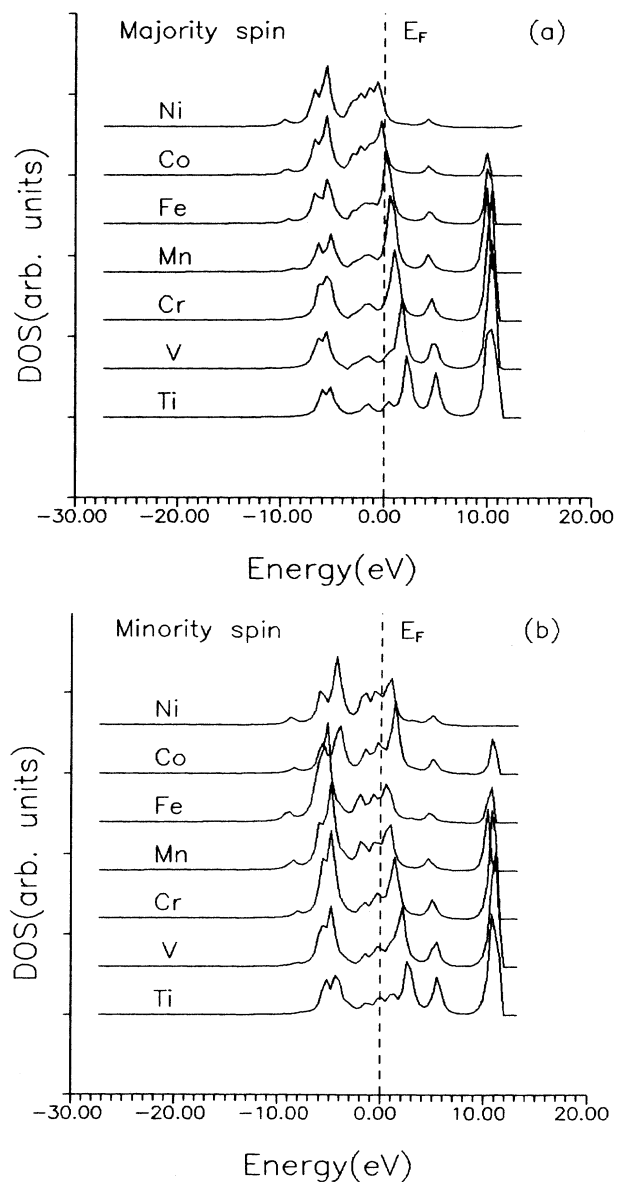


FIG. 4. Partial densities of states (PDOS) for the central  $M$  atom in an icosahedral  $M\text{Co}_{12}$  cluster: (a) majority spin and (b) minority spin.

CoCo<sub>12</sub> cluster as a typical example, whose DOS(↑) and DOS(↓) are separately shown in Fig. 3. From Fig. 3, we see that there are five peaks in the valence band of the CoCo<sub>12</sub> cluster. They are almost in one-to-one correspondence with those calculated by Moruzzi, Janak, and Williams<sup>23</sup> for a fcc Co crystal and by McHenry *et al.*<sup>27</sup> for an icosahedral CoCo<sub>12</sub> cluster with the Co-Co bond length taken as that in bulk Co. However, there are differences in the shape and position of the peaks. Mulliken population analysis<sup>28</sup> indicates that peaks *A*–*C* are dominantly of *d* character, peak *D* is of *spd* hybrid character, and peak *E* is of *sp* hybrid character. Comparing the DOS(↑) and DOS(↓) in Fig. 3, we estimate the exchange splitting to be 1.8 eV for the CoCo<sub>12</sub> cluster. This value is bigger than 1.5 eV of McHenry *et al.*<sup>27</sup> for the CoCo<sub>12</sub> cluster, and close to 1.7 eV of Marcus and Moruzzi<sup>29</sup> and for a fcc Co crystal.

Let us now return to Fig. 2 to examine the effect of *M* on the DOS for *M*Co<sub>12</sub> clusters. With the central atom *M* changing from Ti to Ni, one can see that the peaks below *E<sub>F</sub>* in Fig. 2(a) move down gradually while they do not change their positions in Fig. 2(b). This is to say that the exchange splitting of a cluster becomes larger with the increase of the atomic number of the central atom *M*.

Figure 4 shows the partial DOS for the *M* atoms in *M*Co<sub>12</sub> clusters. From Fig. 4(a), we see that the peaks of M3*d* shift toward the lower bands and

meanwhile the crystal-field splitting deduces monotonically with *M* changing from Ti to Ni.

Table II lists some numerical results on the electronic structure of *M*Co<sub>12</sub> clusters. The gap between the highest occupied molecular orbital (HOMO) and the lowest unoccupied molecular orbital (LUMO) is found to be rather small for all *M*Co<sub>12</sub> clusters, indicating that all *M*Co<sub>12</sub> clusters are metallic in behavior. The values of *E<sub>F</sub>*, *E<sub>HOMO</sub>*, and *E<sub>LUMO</sub>* vary very little with *M*, but the valence-band width (VBW) is found to depend on *M*. The VBW becomes wider with an increase in the atomic number of *M* except for that of VCo<sub>12</sub>. The VBW of the CoCo<sub>12</sub> cluster is 9.36 eV. This value, similar to that of the exchange splitting, is bigger than the 7.0 eV of McHenry *et al.*<sup>27</sup> for the CoCo<sub>12</sub> cluster, and close to the 9.0 eV of Marcus and Moruzzi<sup>29</sup> for a fcc Co crystal.

Table III gives the ground-state electronic configurations for *M*Co<sub>12</sub> clusters. As has already been seen in Fig. 2(b), all HOMO's are occupied by the minority-spin electrons. The HOMO's for TiCo<sub>12</sub>, MnCo<sub>12</sub>, and CoCo<sub>12</sub> are fully occupied, which lead to ground states with closed electronic shells. These clusters are thus remarkably stable. The rest of the *M*Co<sub>12</sub> clusters (*M* = V, Cr, Fe, and Ni) have open electronic shells because their HOMO's are partially occupied. These clusters with open electronic shells have degenerate ground states. According to the Jahn-Teller theorem,

TABLE IV. Mulliken populations for atomic orbitals of icosahedral *M*Co<sub>12</sub> clusters.

Cluster	Orbital	Charge	
		Center atom	Surface atom
TiCo <sub>12</sub>	3 <i>d</i>	2.431	7.386
	4 <i>s</i>	0.652	0.721
	4 <i>p</i>	2.015	0.802
	effective charge	−1.098	+0.091
VCo <sub>12</sub>	3 <i>d</i>	3.413	7.391
	4 <i>s</i>	0.657	0.737
	4 <i>p</i>	1.798	0.799
	effective charge	−0.868	+0.072
CrCo <sub>12</sub>	3 <i>d</i>	4.765	7.370
	4 <i>s</i>	0.740	0.656
	4 <i>p</i>	2.006	0.848
	effective charge	−1.511	+0.126
MnCo <sub>12</sub>	3 <i>d</i>	5.211	7.378
	4 <i>s</i>	0.885	0.714
	4 <i>p</i>	1.946	0.821
	effective charge	−1.042	+0.087
FeCo <sub>12</sub>	3 <i>d</i>	6.223	7.383
	4 <i>s</i>	0.904	0.701
	4 <i>p</i>	1.918	0.829
	effective charge	−1.045	+0.087
CoCo <sub>12</sub>	3 <i>d</i>	7.280	7.364
	4 <i>s</i>	0.856	0.755
	4 <i>p</i>	1.933	0.792
	effective charge	−1.069	+0.089
NiCo <sub>12</sub>	3 <i>d</i>	8.269	7.362
	4 <i>s</i>	0.889	0.741
	4 <i>p</i>	1.882	0.810
	effective charge	−1.040	+0.087

they tend to distort further toward lower symmetry so as to lift the degeneracy of their ground states and lower their energies.<sup>30</sup> It should be pointed out, however, that the distorted cluster may also increase its energy if it possesses a decreased spin. Accordingly, it depends on a compromise between two such effects whether or to what extent the Jahn-Teller distortion may take place.

Table IV lists the Mulliken populations for atomic orbitals of  $M\text{Co}_{12}$  clusters. From this table, we see that the central  $M$  atoms have negative effective charges and that surface Co atoms have positive charges in all clusters. This means that the central  $M$  atom obtains electrons from surface Co atoms. A further analysis indicates that there is another way to obtain charge transfer in clusters. That is, electrons transfer between two atomic orbitals of an atom. For all clusters except  $\text{CrCo}_{12}$ , there are electron transfers from  $M4s$  to  $M3d$ ,  $M4s$  to  $M4p$ ,  $\text{Co}4s$  to  $\text{Co}3d$ , and  $\text{Co}4s$  to  $\text{Co}4p$ . In  $\text{CrCo}_{12}$ , however,  $\text{Cr}3d$  does not obtain but rather loses electrons. The anomaly in the charge transfer of  $\text{Cr}3d$  might be attributed to the particular electronic configuration of the free Cr atom ( $\text{Cr}3d^5 4s^1$ ).

Table V lists the total and local magnetic moments of the  $M\text{Co}_{12}$  clusters. In  $\text{CoCo}_{12}$  and  $\text{NiCo}_{12}$  clusters, the moments of the central atoms align in parallel to those of

the surface atoms, so they have ferromagnetic (FM) interactions. The other  $M\text{Co}_{12}$  clusters ( $M = \text{Ti}, \text{V}, \text{Cr}, \text{Mn}$ , and  $\text{Fe}$ ) are antiferromagnetic (AFM), where the moments of the central and surface atoms align in opposite directions. It is worth noticing that the magnetic interaction between Fe and Co atoms is AFM, which is in contrast with the well-known FM interaction in Fe-doped Co metal. Besides, even in FM  $\text{CoCo}_{12}$  and  $\text{NiCo}_{12}$  clusters, the local moment of  $M3d$  aligns antiferromagnetically with those of  $M4s$  and  $M4p$ .

Among  $M\text{Co}_{12}$  clusters,  $\text{CoCo}_{12}$  has the largest moment ( $31 \mu\text{B}$ ), of which the surface Co atom has a moment of  $2.42 \mu\text{B}$ , 24% larger than that of the central atom ( $1.95 \mu\text{B}$ ). The total magnetic moment of the cluster is reduced by the substitution of the central Co atom with  $M$ . Nonetheless, the average moments of all clusters are obviously larger than that of the fcc Co crystal ( $1.56\text{--}1.66 \mu\text{B}/\text{atom}$ ).<sup>24,29,31</sup> This result can be understood by noticing the fact that the magnetic moment of a FM solid can be enhanced by reducing the dimensionality<sup>32</sup> and that a large fraction of atoms in a cluster are surface atoms.

With the LSD transition-state theory, we calculate the ionization potentials (IP's) for all  $M\text{Co}_{12}$  clusters. The results are presented in Table VI. From Table VI, we

TABLE V. Magnetic properties of icosahedral  $M\text{Co}_{12}$  clusters ( $\mu\text{B}$ ). CSI denotes the type of interaction between the central and surface atoms.

Cluster	Orbital	Local moment ( $\mu\text{B}$ )		CSI	Total moment
		Center atom	Surface atom		
$\text{TiCo}_{12}$	$3d$	-0.577	2.156	AFM	26
	$4s$	-0.184	0.002		
	$4p$	-0.270	0.095		
	total	-1.031	2.253		
$\text{VCo}_{12}$	$3d$	-0.786	2.086	AFM	25
	$4s$	-0.163	0.000		
	$4p$	-0.153	0.089		
	total	-1.102	2.175		
$\text{CrCo}_{12}$	$3d$	-1.158	2.076	AFM	24
	$4s$	-0.179	-0.007		
	$4p$	-0.115	0.052		
	total	-1.452	2.121		
$\text{MnCo}_{12}$	$3d$	-1.974	2.099	AFM	23
	$4s$	-0.237	0.025		
	$4p$	-0.287	0.000		
	total	-2.498	2.124		
$\text{FeCo}_{12}$	$3d$	-1.781	2.015	AFM	22
	$4s$	-0.212	0.006		
	$4p$	-0.222	-0.003		
	total	-2.215	2.018		
$\text{CoCo}_{12}$	$3d$	2.266	2.251	FM	31
	$4s$	-0.117	0.006		
	$4p$	-0.197	0.163		
	total	1.953	2.420		
$\text{NiCo}_{12}$	$3d$	1.361	2.258	FM	30
	$4s$	-0.154	0.020		
	$4p$	-0.157	0.141		
	total	1.050	2.419		

TABLE VI. Ionization potentials for icosahedral  $M\text{Co}_{12}$  clusters.

Cluster	TiCo <sub>12</sub>	VCo <sub>12</sub>	CrCo <sub>12</sub>	MnCo <sub>12</sub>	FeCo <sub>12</sub>	CoCo <sub>12</sub>	NiCo <sub>12</sub>
<i>I</i> (eV)	5.58	5.57	5.41	5.46	5.38	5.73	5.56

could not find an obvious relationship between the IP and  $M$ . The IP for CoCo<sub>12</sub> is 5.73 eV, which is slightly larger than all other  $M\text{Co}_{12}$  clusters, and agrees with the experimental value<sup>12</sup> of 5.74 eV.

### C. Reactivity of $M\text{Co}_{12}$ clusters toward H<sub>2</sub>, N<sub>2</sub>, and CO molecules

The reactivity of metal catalysts toward gaseous molecules has been a subject of great scientific and technological interest and most catalytically active metals are in the transition group.<sup>33–34</sup> Since the catalytic reaction takes place around the metal surface, the surface properties play an important role. There are three main types<sup>34</sup> of metal surfaces whose catalytic activity has been investigated. The first type is a bulk sample, usually in the form of a single-crystal surface or a fine wire; the second type of surface is an evaporated metal film; and the third, which is by far the most important type of catalyst for industrial processes, consists of small particles of metal supported on a finely divided oxide powder. For the last type of catalyst, small particles with high dispersity are desirable because they maximize the fraction of the metal exposed as surface atoms. Since clusters and cluster-assembled small particles consist largely of surface atoms and are distinct from their bulk counterparts in the geometrical and electronic structures, the study of the influence of cluster size and electronic properties on catalytic activity has attracted wide attention.<sup>13–16</sup>

It is believed that chemisorption of a molecule on the metal catalyst is the first step in the catalytic reaction. Therefore, it is important to study first the mechanism of chemisorption. The chemisorption of a molecule on a metal cluster can be regarded as a process of chemical reaction between them. In quantum chemistry, such a bimolecular reaction is described by the frontier orbital theory<sup>35</sup>(FOT) which can be summarized by the following three points.

(a) The frontier orbitals, HOMO and LUMO, of reactant molecules play the leading role in their reaction. When two reactant molecules approach, the HOMO of one molecule should be adapted in symmetry to the LUMO of the other. In other words, suppose that the molecular orbitals of interest are real functions which can be schematically represented by a set of alternating plus and minus lobes in their contour maps. The adaptation in symmetry means that the two interacting frontier orbitals, HOMO and LUMO, should approach in such a direction that leads to the plus-plus and minus-minus overlappings. Overlapping in this way will be nonzero and sufficiently strong so that adsorption can effectively take place.

(b) The interacting HOMO and LUMO in the above reaction should have close energies.

(c) As the reaction proceeds, there will be charge

transfer from the HOMO of one molecule to the LUMO of the other and charge should transfer in such a way that the bonds of the reactant molecules are weakened.

For adsorption to occur favorably, all of the above three points should be satisfied. Let us analyze now the reactivity of the  $M\text{Co}_{12}$  cluster toward H<sub>2</sub>, N<sub>2</sub>, and CO molecules on the basis of our electronic structure results and FOT.

Figure 5 shows schematically the frontier orbitals for H<sub>2</sub>, N<sub>2</sub>, and CO molecules and for  $M\text{Co}_{12}$  clusters. Since frontier orbitals for different  $M\text{Co}_{12}$  clusters are similar in energy, we only draw those for typical CoCo<sub>12</sub> clusters in the figure. From Fig. 5, one can easily see that the energy span ( $\Delta_1$ ) between the HOMO of clusters and the LUMO of molecules is less than the span ( $\Delta_2$ ) between the LUMO of clusters and the HOMO of molecules. For example, the HOMO of H<sub>2</sub> is the  $\sigma_g$  bonding orbital with energy  $\sim -13.6$  eV, and the LUMO of H<sub>2</sub> is the  $\sigma_u$  antibonding orbital with energy  $\sim -0.1$  eV; while the HOMO and LUMO of CoCo<sub>12</sub> are both around  $-3.7$  eV (see Table II). For H<sub>2</sub> adsorption on CoCo<sub>12</sub>,  $\Delta_1$  and  $\Delta_2$  are, respectively, 3.6 and 9.9 eV, thus  $\Delta_1 \ll \Delta_2$ . It follows from point (b) of the FOT that interaction will take place mainly between the HOMO of clusters and the LUMO of molecules. Since the LUMO's for H<sub>2</sub>, N<sub>2</sub>, and CO molecules are all antibonding ( $\sigma_u$ ,  $\sigma_u$ , and  $\pi^*$ , respectively, see Fig. 5), such adsorption processes also satisfy the requirement of point (c) of the FOT.

According to point (a) of the FOT, whether  $M\text{Co}_{12}$  clusters can effectively adsorb H<sub>2</sub>, N<sub>2</sub>, and CO molecules

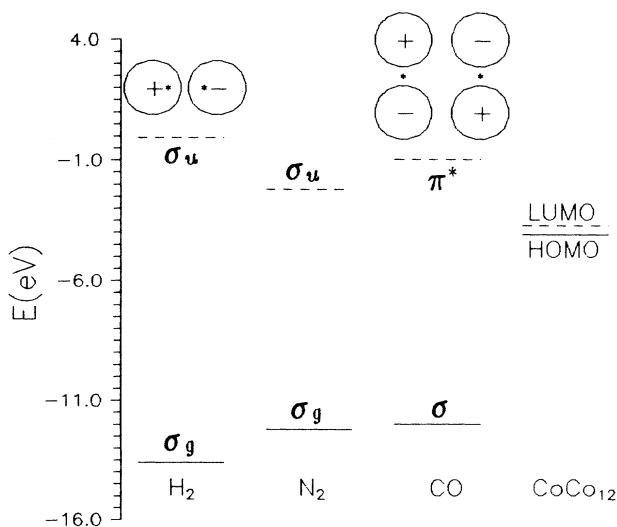


FIG. 5. HOMO's and LUMO's of H<sub>2</sub>, N<sub>2</sub>, and CO molecules and an icosahedral CoCo<sub>12</sub> cluster.

TABLE VII. Orbital populations of HOMO's for icosahedral  $M\text{Co}_{12}$  clusters.  $\text{Co}^{(s)}$  denotes the surface Co atom and other notations are the following:  $p_0 = p_z$ ;  $p_1 = p_x, p_y$ ;  $d_0 = d_{z^2}$ ;  $d_1 = d_{xz}, d_{yz}$ .

Cluster	HOMO	Orbital populations (%)
$\text{TiCo}_{12}$	$2g_u \downarrow$	$27\text{Co}4p_1 + 32\text{Co}3d_1 + 41\text{Co}3d_0$
$\text{VCo}_{12}$	$3t_{1u} \downarrow$	$8\text{V}4p_1 + 9\text{Co}4p_0 + 10\text{Co}4p_1 + 28\text{Co}3d_0$
$\text{CrCo}_{12}$	$3t_{1u} \downarrow$	$8\text{Cr}4p_1 + 10\text{Co}4p_0 + 7\text{Co}4p_1 + 30\text{Co}3d_0 + 45\text{Co}3d_1$
$\text{MnCo}_{12}$	$3t_{1u} \downarrow$	$8\text{Mn}4p_1 + 7\text{Co}4p_0 + 9\text{Co}4p_1 + 27\text{Co}3d_0 + 49\text{Co}3d_1$
$\text{FeCo}_{12}$	$2g_g \downarrow$	$3\text{Co}4p_1 + 92\text{Co}3d_1 + 5\text{Co}3d_0$
$\text{CoCo}_{12}$	$2g_u \downarrow$	$27\text{C}^{(s)}4p_1 + 29\text{Co}^{(s)}3d_1 + 44\text{Co}^{(s)}3d_0$
$\text{NiCo}_{12}$	$3t_{1u} \downarrow$	$7\text{Ni}4p_1 + 6\text{Co}4p_0 + 12\text{Co}4p_1 + 25\text{Co}3d_0 + 50\text{Co}3d_1$

depends on whether the interacting HOMO of the clusters and LUMO of the molecules are symmetry adapted.

The contour maps for the LUMO's of  $\text{H}_2$ ,  $\text{N}_2$ , and  $\text{CO}$  are shown in Fig. 5. They all consist of alternating plus and minus lobes along their bonding axes.

Table VII lists the orbital populations for HOMO's of  $M\text{Co}_{12}$  clusters. We can divide these clusters into three types according to their HOMO character. The first type contains  $\text{FeCo}_{12}$ . Its HOMO is  $2g_g \downarrow$ , which consists dominantly of  $\text{Co}3d_1$  character ( $\sim 92\%$ ) and slightly of  $\text{Co}3d_0$  ( $\sim 5\%$ ) and  $\text{Co}4p_1$  ( $\sim 3\%$ ). The second type contains  $\text{TiCo}_{12}$  and  $\text{CoCo}_{12}$ . Their HOMO's are  $2g_u \downarrow$ , which is composed of 29–33%  $\text{Co}^{(s)}3d_1$ , 41–44%  $\text{Co}^{(s)}3d_0$ , and 27%  $\text{Co}^{(s)}4p_1$ . The rest of the clusters,  $\text{VCo}_{12}$ ,  $\text{CrCo}_{12}$ ,  $\text{MnCo}_{12}$ , and  $\text{NiCo}_{12}$ , belong to the third type. Their HOMO's are  $3t_{1u} \downarrow$ , which has a rather complicated composition, i.e., 45–50%  $\text{Co}3d_1$ , 25–30%  $\text{Co}3d_0$ , 6–10%  $\text{Co}4p_1$ , and, what is more, 7–8%  $4p_1$  of the central  $M$  atom.

Since HOMO's of the same type of clusters have simi-

lar composition and, hence, manifest similar maps and contours, it is sufficient to draw and analyze the maps and/or corresponding contours for the HOMO of just one cluster for each type. Figures 6 and 7 show the maps and corresponding contours for the HOMO of  $\text{FeCo}_{12}$  (of type I) on two typical planes. From these figures, one can see that the HOMO of  $\text{FeCo}_{12}$  consists of many alternating plus and minus lobes. This character is much similar to that of the LUMO's of  $\text{H}_2$ ,  $\text{N}_2$ , and  $\text{CO}$ , indicating that the HOMO of  $\text{FeCo}_{12}$  can match up in symmetry the LUMO of  $\text{H}_2$ ,  $\text{N}_2$ , or  $\text{CO}$ . Thus, the  $\text{FeCo}_{12}$  cluster can effectively adsorb  $\text{H}_2$ ,  $\text{N}_2$ , or  $\text{CO}$  as long as they approach in the direction which corresponds to plus-plus and minus-minus overlappings.

Similar to  $\text{FeCo}_{12}$ , the HOMO of  $\text{CoCo}_{12}$  also consists of a set of alternating plus and minus lobes (Fig. 8); therefore, the adsorption of  $\text{CoCo}_{12}$  toward  $\text{H}_2$ ,  $\text{N}_2$ , and  $\text{CO}$  can effectively take place. A further analysis indicates

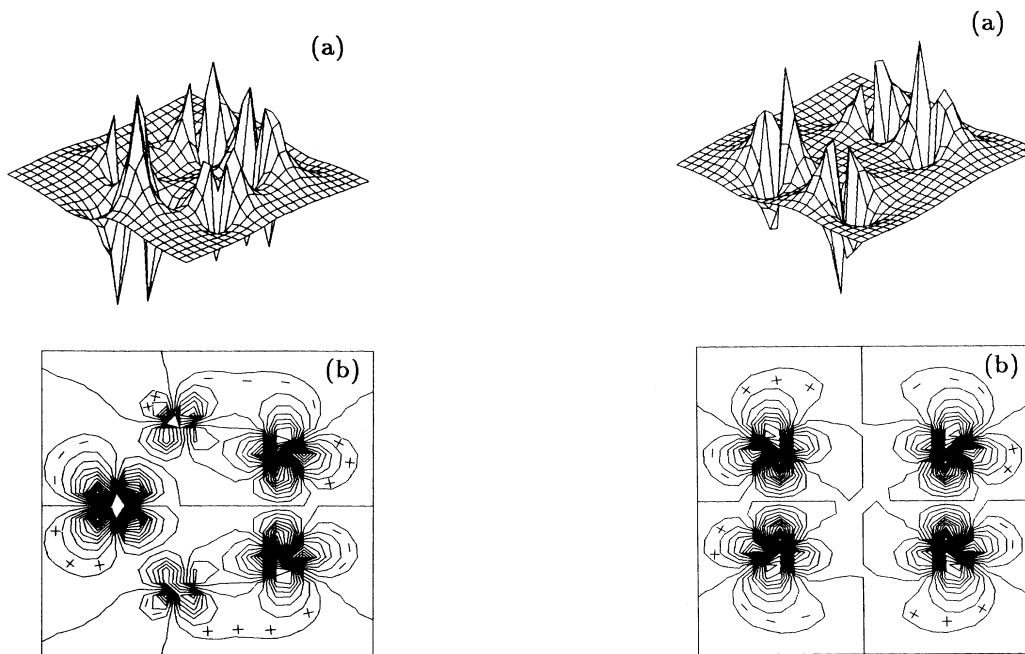


FIG. 6. HOMO of an icosahedral  $\text{FeCo}_{12}$  cluster in the plane passing through the five surface Co atoms (hereafter,  $A$  plane): (a) map and (b) contour.

FIG. 7. HOMO of an icosahedral  $\text{FeCo}_{12}$  cluster in the plane passing through the central  $M$  and four surface Co atoms (hereafter,  $B$  plane): (a) map and (b) contour.

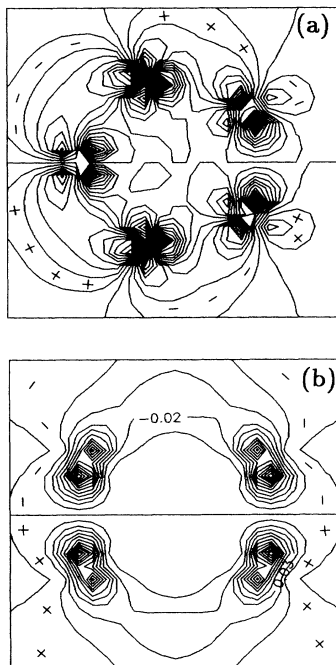


FIG. 8. The contours for the HOMO of an icosahedral  $\text{CoCo}_{12}$  cluster in (a) the  $A$  plane and (b) the  $B$  plane.

that the reactivity of these two types of clusters can be different in strength. As is known, adsorption is a dynamical process, in which the molecules may approach the cluster in random directions. Carefully comparing the HOMO's of  $\text{FeCo}_{12}$  and  $\text{CoCo}_{12}$ , one can find that the HOMO of  $\text{FeCo}_{12}$  contains more plus and minus lobes than  $\text{CoCo}_{12}$  does. As a result, effective overlappings between the HOMO of a cluster and the LUMO of a molecule can appear in more possible directions for  $\text{FeCo}_{12}$  than for  $\text{CoCo}_{12}$ . So, we can say that  $\text{FeCo}_{12}$  has a higher reactivity than  $\text{CoCo}_{12}$  toward  $\text{H}_2$ ,  $\text{N}_2$ , and  $\text{CO}$ .

The HOMO of  $\text{VCo}_{12}$  has only plus or minus lobes between the two nearest-neighbor surface atoms (Fig. 9). Hence, the HOMO of  $\text{VCo}_{12}$  is not symmetry adapted to the LUMO of  $\text{H}_2$ ,  $\text{N}_2$ , and  $\text{CO}$ . Effective overlappings between the HOMO of  $\text{VCo}_{12}$  and the LUMO of  $\text{H}_2$ ,  $\text{N}_2$ , or  $\text{CO}$  would be small and adsorption could hardly occur.

Experimentally, the reactivity of  $\text{CoCo}_{12}$  and  $\text{VCo}_{12}$  clusters toward  $\text{H}_2$ ,  $\text{N}_2$ , and  $\text{CO}$  molecules have been measured.<sup>13–16</sup> The experimental results indicate that  $\text{CoCo}_{12}$  has substantial reactivity, while  $\text{VCo}_{12}$  shows high stability, in agreement with our analyses.

#### IV. SUMMARY

In this paper, we have performed a comprehensive study of  $M\text{Co}_{12}$  clusters on the stability, electronic and magnetic properties, and reactivity toward  $\text{H}_2$ ,  $\text{N}_2$ , and  $\text{CO}$  molecules, using the first-principles DV-LSD method. The results we have obtained can be summarized as follows.

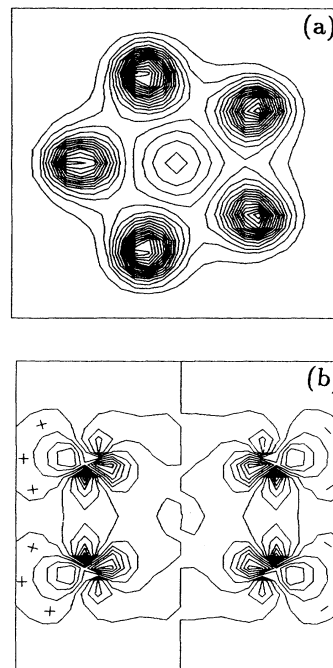


FIG. 9. The contours for the HOMO of an icosahedral  $\text{VCo}_{12}$  cluster in (a) the  $A$  plane and (b) the  $B$  plane.

(1) By the binding-energy calculation, we optimize the  $M$ -Co equilibrium bond lengths in icosahedral  $M\text{Co}_{12}$  clusters. The results indicate that the  $M$ -Co bond lengths are contracted in all of the clusters compared with the summation of radii of free atoms  $M$  and  $\text{Co}$ .

(2) Comparing the binding energies of  $M\text{Co}_{12}$  clusters in their equilibrium configurations, we find that  $\text{CrCo}_{12}$  is the most energetically stable among all the clusters, and that all the rest of the clusters except  $\text{NiCo}_{12}$  are more energetically stable than the  $\text{CoCo}_{12}$  cluster.

(3) The electronic structures of  $M\text{Co}_{12}$  clusters have been calculated. The results reveal that all  $M\text{Co}_{12}$  clusters have metallic characters. Their VBW's increase monotonically with  $M$  running from  $\text{Ti}$  and  $\text{Ni}$  except  $\text{V}$ . The values of  $E_{\text{HOMO}}$ ,  $E_{\text{LUMO}}$ , and  $E_F$  are found to change very little with  $M$ .

(4) The ground-state electronic configurations for  $M\text{Co}_{12}$  clusters are obtained. The HOMO's of  $\text{TiCo}_{12}$ ,  $\text{MnCo}_{12}$ , and  $\text{CoCo}_{12}$  are fully occupied and are, thus, remarkably stable. The  $\text{VCo}_{12}$ ,  $\text{CrCo}_{12}$ ,  $\text{FeCo}_{12}$ , and  $\text{NiCo}_{12}$  clusters have open electronic shells and are expected to distort further according to the Jahn-Teller theorem.

(5) The local and total magnetic properties of  $M\text{Co}_{12}$  clusters are analyzed. The cluster moment is reduced by the substitution of the central  $\text{Co}$  atom with  $M$ . The average moment per atom of all  $M\text{Co}_{12}$  clusters is bigger than that of the bulk  $\text{Co}$ . In addition, the interaction between  $\text{Fe}$  and  $\text{Co}$  is found to be AFM in the  $\text{FeCo}_{12}$  cluster.

(6) With the transition-state theory, we calculate the

ionization potentials of  $M\text{Co}_{12}$  clusters. The result we obtained for  $\text{CoCo}_{12}$  is in excellent agreement with the experiment value.

(7) Based on the results of electronic structures, we analyze the reactivity of  $M\text{Co}_{12}$  clusters toward gaseous molecules. The reactivity of these clusters toward  $\text{H}_2$ ,  $\text{N}_2$ , and  $\text{CO}$  molecules can be classified in three types. The first type includes  $\text{FeCo}_{12}$ , which has a high reactivity. The second type involves  $\text{TiCo}_{12}$  and  $\text{CoCo}_{12}$ , which have

moderate reactivity. The third type contains  $\text{VCo}_{12}$ ,  $\text{CrCo}_{12}$ ,  $\text{MnCo}_{12}$ , and  $\text{NiCo}_{12}$ , which have little reactivity. The results for  $\text{VCo}_{12}$  and  $\text{CoCo}_{12}$  clusters have been confirmed by experiments.

#### ACKNOWLEDGMENT

This work was supported by the National Natural Science Foundation of China.

\*Mailing address.

<sup>1</sup>For a review see, Proceedings of the Fifth International Meeting on Small Particles and Inorganic Clusters [Z. Phys. D **19**, Nos. 1-4 (1991)].

<sup>2</sup>C. Y. Yang, K. H. Johnson, D. R. Salahub, and J. Kaspar, Phys. Rev. B **24**, 5673 (1981).

<sup>3</sup>C. W. Bauschlicher and L. G. M. Pettersson, J. Chem. Phys. **84**, 2226 (1986).

<sup>4</sup>S. Nonose, Y. Chiba, K. Onodera, S. Sudo, and K. Kaya, Chem. Phys. Lett. **164**, 427 (1989).

<sup>5</sup>W. J. C. Menezes and M. B. Knickelbein, Chem. Phys. Lett. **183**, 357 (1991).

<sup>6</sup>L. G. M. Pettersson and C. W. Bauschlicher, Chem. Phys. **131**, 263 (1989).

<sup>7</sup>B. I. Dunlap, Z. Phys. D **19**, 255 (1991).

<sup>8</sup>S. N. Khanna and P. Jena, Phys. Rev. Lett. **69**, 1664 (1992).

<sup>9</sup>D. R. Salahub and R. P. Messmer, Surf. Sci. **106**, 415 (1981).

<sup>10</sup>M. R. Zapkin, D. M. Cox, R. O. Brickman, and A. J. Kaldor, J. Phys. Chem. **93**, 6823 (1989).

<sup>11</sup>A. Vega, J. Dorantes-Davila, G. M. Pastor, and L. C. Balbas, Z. Phys. D **19**, 263 (1991).

<sup>12</sup>S. Yang and M. B. Knickelbein, J. Chem. Phys. **93**, 1533 (1990).

<sup>13</sup>M. D. Morse, M. E. Geusic, J. R. Health, and R. E. Smalley, J. Chem. Phys. **83**, 2293 (1985).

<sup>14</sup>D. M. Cox, K. C. Riechmann, D. J. Trevor, and A. J. Kaldor, J. Chem. Phys. **88**, 111 (1988).

<sup>15</sup>S. Nonose, Y. Sone, K. Onodera, S. Sudo, and K. Kaya, J. Chem. Phys. **94**, 2744 (1990).

<sup>16</sup>S. Nonose, Y. Sone, and K. Kaya, Z. Phys. D **19**, 357 (1991).

<sup>17</sup>L. G. M. Peterson and C. W. Bauschlicher, J. Chem. Phys. **87**, 2205 (1987).

<sup>18</sup>Yang Jinlong, Xia Shangda, and Wang Kelin, Chin. J. Chem. Phys. **3**, 436 (1990).

<sup>19</sup>B. Delley, D. E. Ellis, A. J. Freeman, E. J. Baerends, and D. Post, Phys. Rev. B **27**, 2132 (1983).

<sup>20</sup>Yang Jinlong, Wang Kelin, L. F. Donà dalle Rose, and F. Toigo, Phys. Rev. B **44**, 4275 (1991); **44**, 10 508 (1991).

<sup>21</sup>D. Guenzburger and D. E. Ellis, Phys. Rev. B **45**, 285 (1992).

<sup>22</sup>V. von Barth and L. Hedin, J. Phys. C **5**, 1629 (1972).

<sup>23</sup>V. L. Moruzzi, J. F. Janak, and A. R. Williams, *Calculated Electronic Properties of Metals* (Pergamon, New York, 1978).

<sup>24</sup>J. F. Janak, Solid State Commun. **25**, 53 (1978).

<sup>25</sup>G. Apai, J. F. Hamilton, J. Stohr, and A. Thompson, Phys. Rev. Lett. **43**, 165 (1979).

<sup>26</sup>D. E. Ellis, G. A. Benesh, and E. Byrom, Phys. Rev. B **20**, 1198 (1979).

<sup>27</sup>M. E. McHenry, M. E. Eberhart, R. C. O'handley, and K. H. Johnson, J. Magn. Magn. Mater. **54-57**, 279 (1986).

<sup>28</sup>R. S. Mulliken, J. Chem. Phys. **23**, 1833 (1955).

<sup>29</sup>P. M. Marcus and V. L. Moruzzi, Solid State Commun. **55**, 971 (1985).

<sup>30</sup>M. E. Eberhart, R. C. O'handley, and K. H. Johnson, Phys. Rev. B **29**, 1097 (1984).

<sup>31</sup>B. I. Min, T. Oguchi, and A. J. Freeman, Phys. Rev. B **33**, 7852 (1986).

<sup>32</sup>F. Lin, M. R. Press, S. N. Khana, and P. Jena, Phys. Rev. B **39**, 6914 (1989).

<sup>33</sup>R. P. H. Gasser, *An Introduction to Chemisorption and Catalysis by Metals* (Clarendon, Oxford, 1985), Chap. 8.

<sup>34</sup>G. C. Bond, *Heterogeneous Catalysis* (Clarendon, Oxford, 1987), 2nd ed.

<sup>35</sup>K. Fukui, Acc. Chem. Res. **4**, 57 (1971).